Shahrood University of Technology

Iranian Society of Mining Engineering (IRSME)

Journal of Mining and Environment (JME)

journal homepage: www.jme.shahroodut.ac.ir

THOMSON REUTERS

Vol. 10, No. 3, 2019, 717-727.

DOI: 10.22044/jme.2019.8132.1680

A finite element model to simulate magnetic field distribution and laboratory studies in wet low-intensity magnetic separator

P. Karimi[1], A. Khodadadi Darban[1*] and Z. Mansourpour[2]

1. Mining Engineering Department, Tarbiat Modares University, Tehran, Iran
2. School of Chemical Engineering, College of Engineering, University of Tehran, Tehran, Iran

Received 23 February 2019; received in revised form 22 June 2019; accepted 25 June 2019

Keywords

Magnetic Separation

Wet Drum Magnetic Separator

Magnetic Field Simulation

Finite Element Method

Abstract

Low-intensity magnetic separators are widely used in the research works and the industry. Advancement in the magnetic separation techniques has led to an expansion in the application of this method in different fields such as enrichment of magnetic mineral, wastewater treatment, and medicine transfer in the human body. In the mineral processing industry, the main application of wet magnetic separation is via drum separators. The design of this separator is based on drum rotation inside a tank media, where a permanent magnet placed inside the drum as an angle form produces a magnetic field. In the present work, the magnetic variables involved (magnetic flux density, intensity of magnetic field, and gradient of magnetic field intensity) were simulated in the drum wet low-intensity magnetic separator using the finite element method and a COMSOL Multiphysics simulator; these variables were further validated through the measured data. A comparison between the simulation and laboratory measurements (of the magnetic field) showed that the mean value of the simulation error in 94 points in 2 sections was equal to 9.6%. Furthermore, the maximum simulation error in the middle of the magnets, as the most important part of the magnetic field distribution in the process of magnetic separation, was in the 6th direction and equal to 7.8%. Therefore, the performed simulation can be applied as a first step to design and construct more advanced magnetics separators.

1. Introduction

The demand for effective, clean, and simple separation techniques is increasing, while declining mineral resources and environmental restrictions have become more stringent. Since magnetic separation is clean and proceeds at numerous conditions, it has been preferred over other separation techniques in many situations [1], and has led to its unique position among the separation technologies.

Magnetic separations have, for decades, been applicable processes in different industries ranging from steel production to coal desulfurization [2]. Magnetic separation has been used for separation of gangue from ore to enrich low-grade ores [3-8], separation of magnetic from non-magnetic waste [9, 10], heavy media separation [11], separation of pyrite (FeS_2) from coal for desulfurization [2], kaolin (clay) decolorization and removing ironic impurities [2, 12], processing a rare earth mineral deposit [13, 14], water treatment and metal removal [2], waste water treatment [15], food industry and removing rare earth elements [2], etc. Furthermore, in the field of biotechnology such as protein and DNA purification, cell separation, separation of biological cells and drug delivery [2, 10, 16], and biocatalysis and diagnostics, magnetic separation has had a wide range of usage.

According to the different parameters (consisting of intensity of magnetic field, its gradient, and dry or wet operation of the equipment), magnetic separators have been classified as dry

Corresponding author: akdarban@modares.ac.ir (A. Khodadadi Darban).

low-intensity magnetic separators, wet low-intensity magnetic separators, dry high-intensity magnetic separators, wet high-intensity high-gradient magnetic separators, and finally, Eddy-current separators and separation in a magnetic fluid [17]. In another classification, the magnetic separation equipment for mineral processing generally falls into three basic categories: low-, medium-, and high-intensity, based on the relative magnetic field strength employed to accomplish separation [18]. By far, the most frequently used wet low-intensity magnetic separators are drum separators [9, 19]. These separators are used mainly for concentration of strongly magnetic ores (such as magnetite) and recovery of the heavy media (such as magnetite or ferrosilicon) used in dense medium separation [9, 19, 20]. It is probably true to say that the magnets are the heart of the wet drum magnetic separators. In terms of wet drum magnetic separators, the permanent magnets installed inside the drum generate an external magnetic field of a strength that is dependent on the intensity of the magnets. Most wet drum magnetic separators are of the type with ceramic ferrite magnets generating a field strength between 1500 and 2500 gauss [20].

The magnetic separation process has been simulated in limited devices. The majority of these simulations are related to the HGMS equipment and using the CFD numerical method [1, 21-27]. This is while only one simulation study was conducted for the wet LIMS device. In the mentioned study, the flow of materials in the LIMS device was simulated using a combination of the FEM and CFD numerical methods [28].

The first step in simulating the magnetic separation process is to simulate the magnetic field and the corresponding variables. The most accurate numerical method for simulating magnetic variables is the finite element numerical method (FEM) [29-33]. There are several available FEM-based simulators such as COMSOL Multiphysics, Opera, Faraday, and EMAG, which can be successfully used to calculate the magnetic field parameters [28].

In this work, a laboratory wet low-intensity magnetic separator (LIMS) device was primarily disassembled. Next, through the use of the reverse engineering process, the mechanical and magnetic information of the magnets inside the drum was extracted. The magnetic variables of magnetic flux density (B) and magnetic field intensity (H) were then simulated using the finite element method (FEM) and a COMSOL Multiphysics simulator. In the next step, the gradient of magnetic field intensity (∇H) was generated via the Helmholtz math model in the COMSOL Multiphysics simulator. Ultimately, the results of the simulation and laboratory measurements (of the magnetic field) were compared so as to validate the results of the simulation.

2. Material and methods

2.1. Separator device and measuring instrument

In the present work, a wet low magnetic separator device (BOXMAG-Rapid Limited model) was used to simulate the magnetic variables involved in a wet low-intensity magnetic separator. This device contains three main parts, namely a magnetic cylinder, a magnetic sector (consisting of permanent magnets placed in the cylinder in angle form), and a tank (the main position of magnetic separation). It is of note that in the device, magnets are placed in an axial arrangement. Besides, the magnetic sector is comprised of three ferrite types (ceramic rectangular cube block magnets with similar upper and bottom magnets). Figure 1 shows the magnetic separator device, magnets, and 3D initial model. The cylindrical drum and separator tank are steel (316). The remnant magnetization (with the Gaussian unit, a characteristic of the permanent magnet) of all three magnets was 1,500 gauss. The magnetic field values were measured using a gauss-meter (F.W. Bell (SYPRIS), Model 5170) around the magnetic sector of the device at different distances and directions.

2.2. Simulation method and modeling theory

The maps of the magnetic sector, magnetic cylinder, and tank were prepared in the SolidWorks software. Simulation of the magnetic variables was performed through FEM numerical modeling in the COMSOL Multiphysics simulator by the AC/DC module and the Magnetic Fields, No Current options.

In a magnetic separator, when a particle is exposed to an external magnetic field (resulting from the arrangement of permanent magnets), the magnetic force applied to the magnetic field is the main force input in the particle, which is in opposition to the gravity and drag forces [20, 34-36]. The magnetic force applied to the particles carried by the fluid flow (in the magnetic field of the permanent magnet) is a function of the particle magnetization and the gradient of the magnetic field, calculated by Eq. 1.

$$\overrightarrow{F_M} = \mu_0 V_m M \nabla H \quad (1)$$

where μ_0 is the permeability magnetic coefficient in a vacuum ($4\pi \times 10^{-7}$ Tm/A), Vm is the volume of particles, M is the magnetization with Am^{-1} unit, H is the intensity of magnetic field, and finally, (∇H) is the gradient of magnetic field intensity [24, 28, 36].

Therefore, the gradient of the magnetic field should be determined in order to calculate the magnetic force. In a COMSOL Multiphysics simulator, the AC/DC module and the Magnetic Fields, No Current options, are used to simulate the magnetic variables of permanent magnets. In this method, the basic equations used for solving the magnetic field are based on Eqs. 2 and 3 [37]:

$$\nabla.(\mu_0 \mu_r H) = 0 \quad (2)$$

$$H = -\nabla V_m + H_b \quad (3)$$

After calculating the value of magnetic field intensity in different detections, the gradient of magnetic field intensity was quantitatively calculated in the x, y, and z-directions and different points. The gradient of the magnetic field intensity was calculated via Eq. 4. These calculations were performed in the COMSOL Multiphysics simulator using the Helmholtz mathematical model [37].

$$\nabla H = \left(\frac{\partial}{\partial x}, \frac{\partial}{\partial y}, \frac{\partial}{\partial z}\right)\left(H_x, H_y, H_Z\right)$$

$$\nabla H = \begin{bmatrix} \frac{\partial H_x}{\partial x} & \frac{\partial H_x}{\partial y} & \frac{\partial H_x}{\partial z} \\ \frac{\partial H_y}{\partial x} & \frac{\partial H_y}{\partial y} & \frac{\partial H_y}{\partial z} \\ \frac{\partial H_z}{\partial x} & \frac{\partial H_z}{\partial y} & \frac{\partial H_z}{\partial z} \end{bmatrix} = \begin{bmatrix} H_{xx} & H_{xy} & H_{xz} \\ H_{yx} & H_{yy} & H_{yz} \\ H_{zx} & H_{zy} & H_{zz} \end{bmatrix}$$

$$\begin{aligned} \nabla H_x &= H_{xx} + H_{yx} + H_{zx} \\ \nabla H_y &= H_{xy} + H_{yy} + H_{zy} \\ \nabla H_z &= H_{xz} + H_{yz} + H_{zz} \end{aligned} \quad (4)$$

3. Simulation steps

In order to simulate the magnetic variables in the COMSOL Multiphysics, the steps mentioned in Figure 2 were followed.

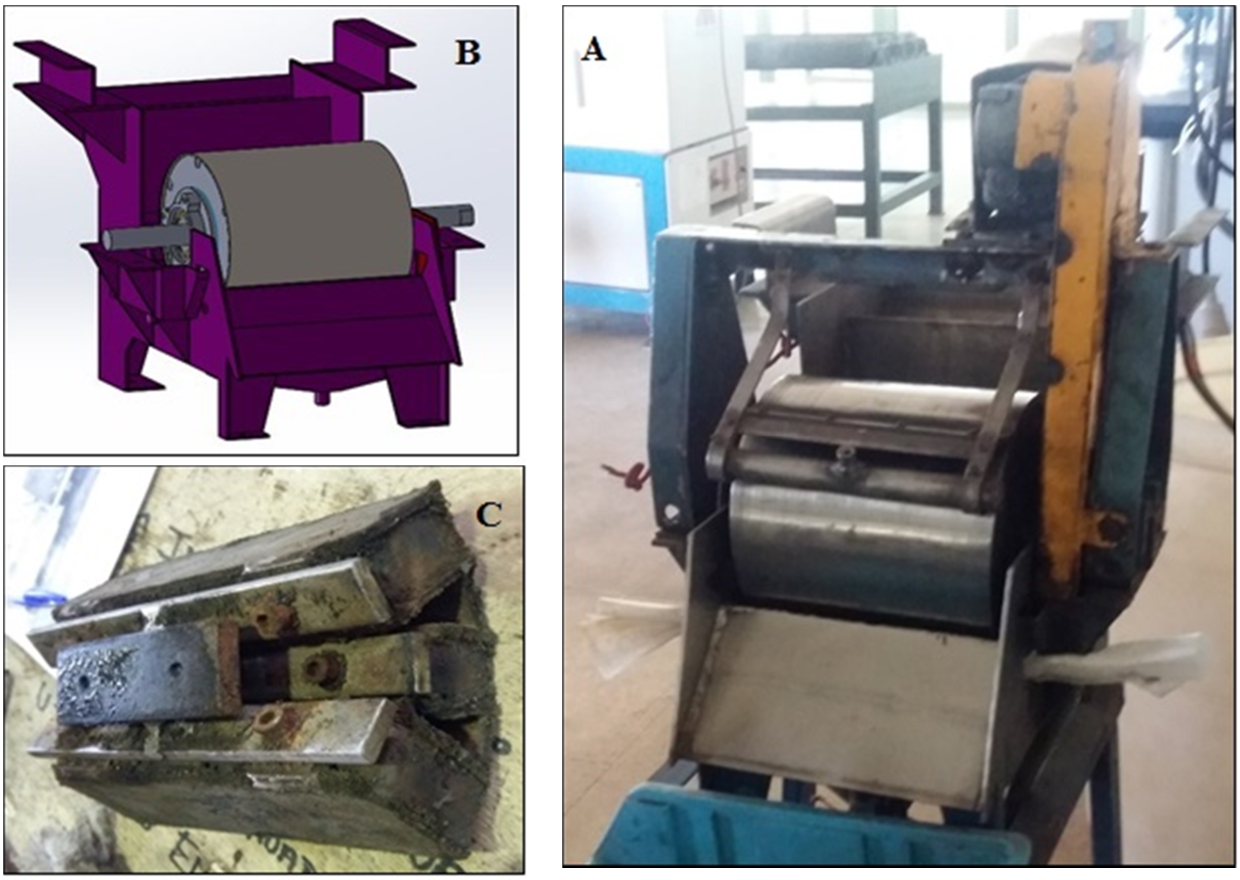

Figure 1. Schematic representation of the wet LIMS device (A), initial 3D model (B), and magnets (C).

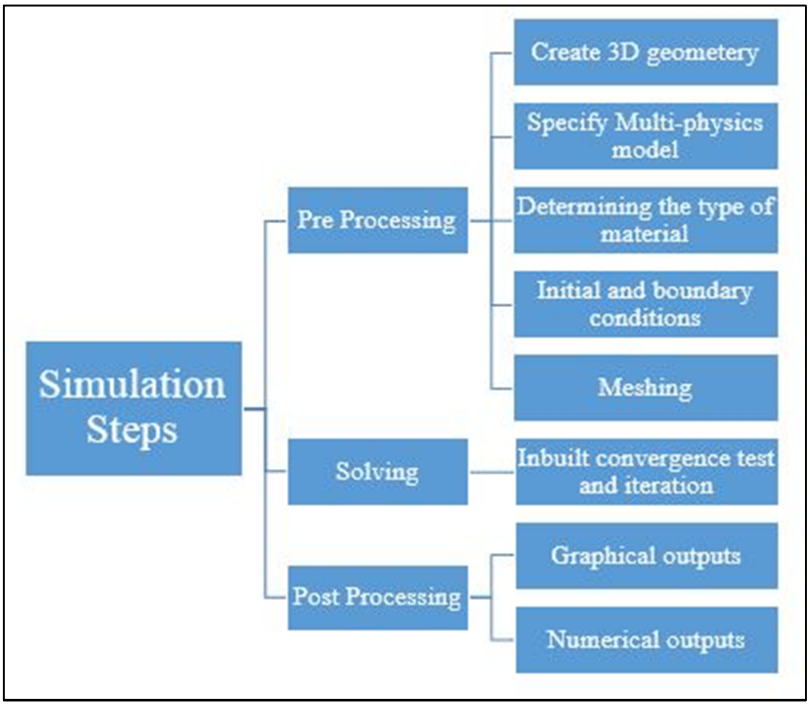

Figure 2. Flow diagram of the simulation steps of magnetic variables in COMSOL Multiphysics.

The following steps are discussed in details in the following sections.

3.1. Determining physics, materials, and geometry criteria

In order to simulate the magnetic field resulting from permanent magnet in COMSOL Multiphysics, the AC/DC module, and the Magnetic Fields, No Current option, was used. In the considered problem, there exist three elements, namely ferrite (ceramic) cuboid magnets, steel cylindrical drum and separator tank (steel 316), and the air covering the magnets. To simulate the magnetic field further employed, were three block-shaped magnets with certain dimensions and arrangements, a steel cylindrical drum (with magnets mounted on the inner shaft), and a separator tank. Figure 3 shows a schematic view of the geometry created in the simulator, COMSOL Multiphysics.

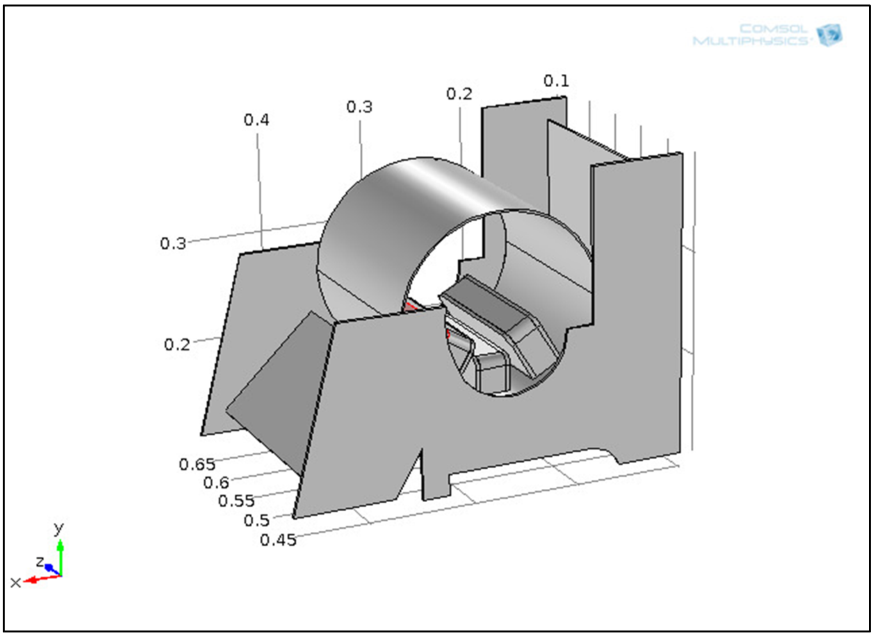

Figure 3. Schematic view of the created geometry of the wet LIMS in the COMSOL Multiphysics (dimension is based on the meter).

3.2. Boundary conditions

In this step, the region related to the generation of the magnetic field was to be specified. The generation power of the magnetic field was also determined using the remnant magnetization variable (1,500 gauss for each one of the three magnets). This value should be applied in a particular direction, referred to as the polarization direction, and determined by the N and S poles of the magnets. In the desired problem, this direction was determined after determining the N and S poles of the magnets and the angle of the magnets with the horizon (X-axis) (Figure 4). Moreover, the magnetic insulation boundary condition was considered as surrounding cubic plates, which limited the calculation of the magnetic field in this space.

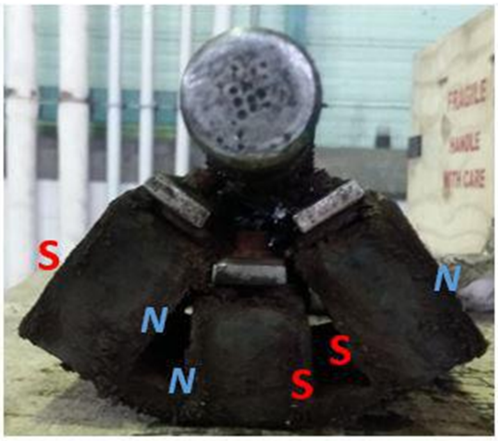

Figure 4. Position of the poles (N and S) in the magnets of the wet LIMS.

3.3. Mesh generation

In general, to create a mesh in the COMSOL simulator, a certain amount of each element is determined by considering the type of the physics. It is possible to use a finer mesh element to reach a higher precision or to reduce the computational size by adopting a larger mesh size. Figure 5 illustrates a view of the constructed mesh where the inlet of the separator is located on the left, and the rotating cylinder shell of the separator is further characterized by a blue circular dense mesh. In this figure, the position of the magnets is also determined and their colored spectrum, according to the legend, indicates the distribution of the magnetic flux density in the space around the magnets. The most important point is that triangular meshes are used so as to achieve a better convergence and stability in the solution.

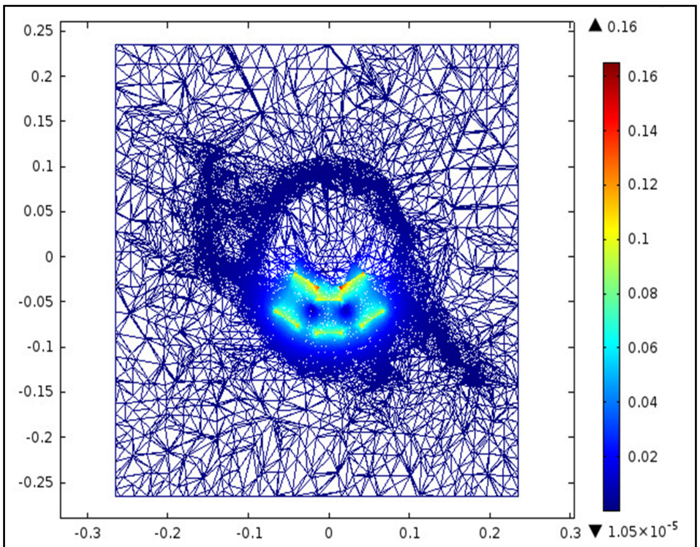

Figure 5. Schematic view of the created mesh with the magnetic flux density distribution in the device.

4. Results and discussion

4.1. Simulation of magnetic flux density (B)

After solving the physics of the problem, the graphical results of the magnetic flux density were shown in Figure 6. As observed, the magnetic flux density value on the magnet was 900 to 1000 gauss, considering the legend on the right side of the figure.

4.2. Simulation of magnetic field intensity (H)

Given that the main purpose of the simulation is to determine H and the gradient of magnetic field intensity, Figures 7, 8, and 9 indicate the values for the magnetic field intensity in the x, y, and z directions.

In addition to the graphical results (Figures 6, 7, and 8), the values (Hx, Hy, Hz) for the various coordinates (x, y, z) are also quantitatively available. Following the calculation of H in various directions, the gradient of the magnetic field intensity was further calculated in different directions (x, y, z) using the Helmholtz model by the COMSOL Multiphysics simulator.

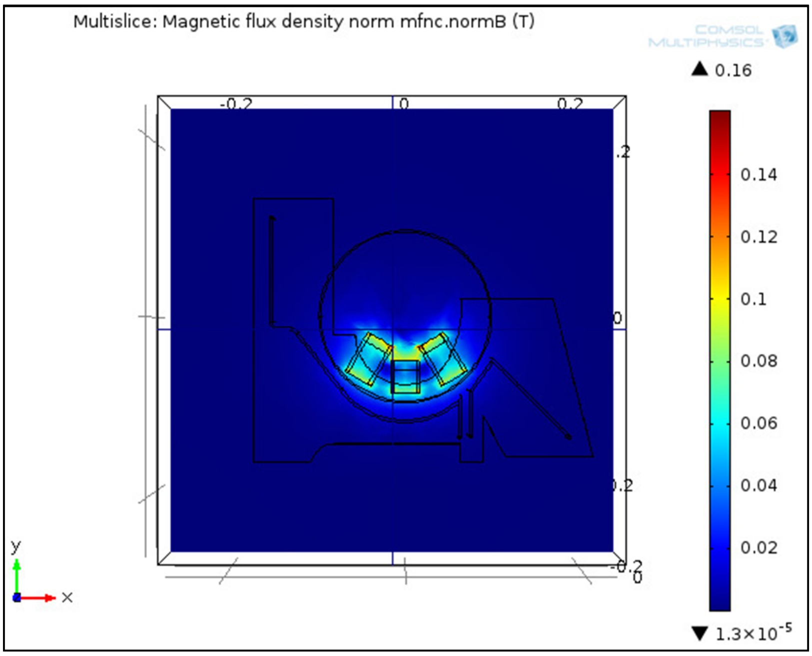

Figure 6. Schematic view of magnetic flux density (Tesla) around the permanent magnets (cylinder and separator tank).

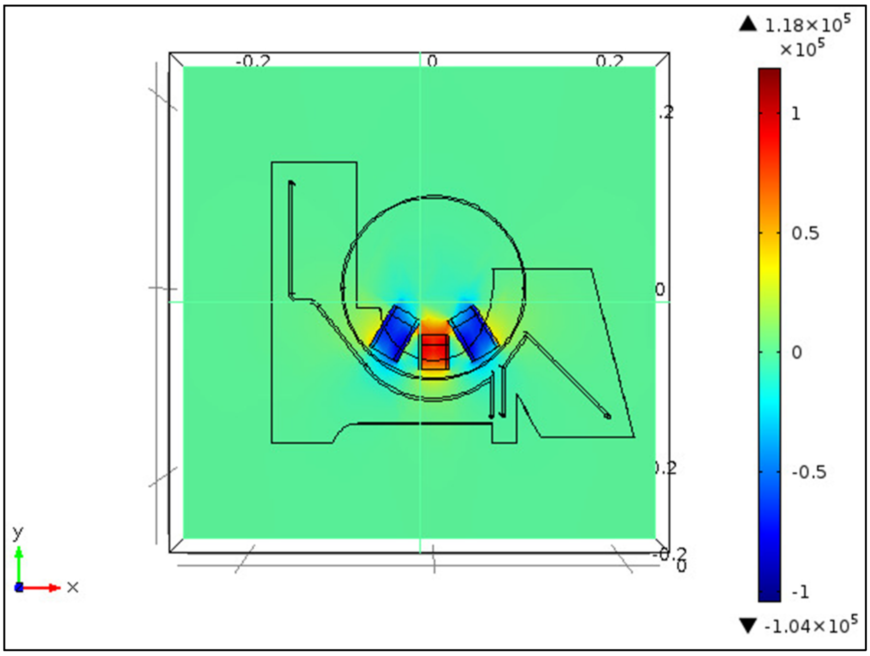

Figure 7. Changes in the magnetic field intensity value in the x-direction (Hx) in wet LIMS device.

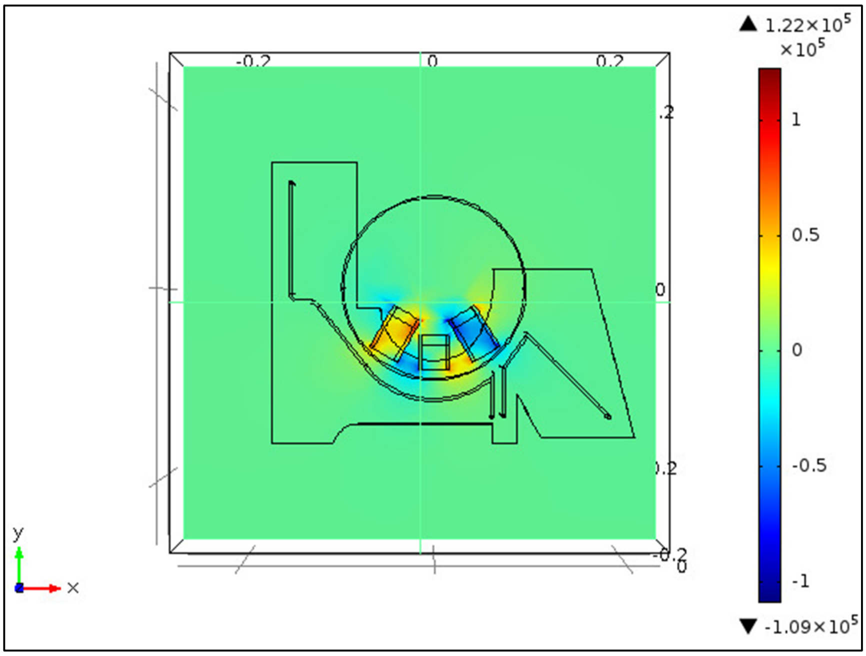

Figure 8. Changes in the magnetic field intensity value in the y-direction (Hy) in wet LIMS device.

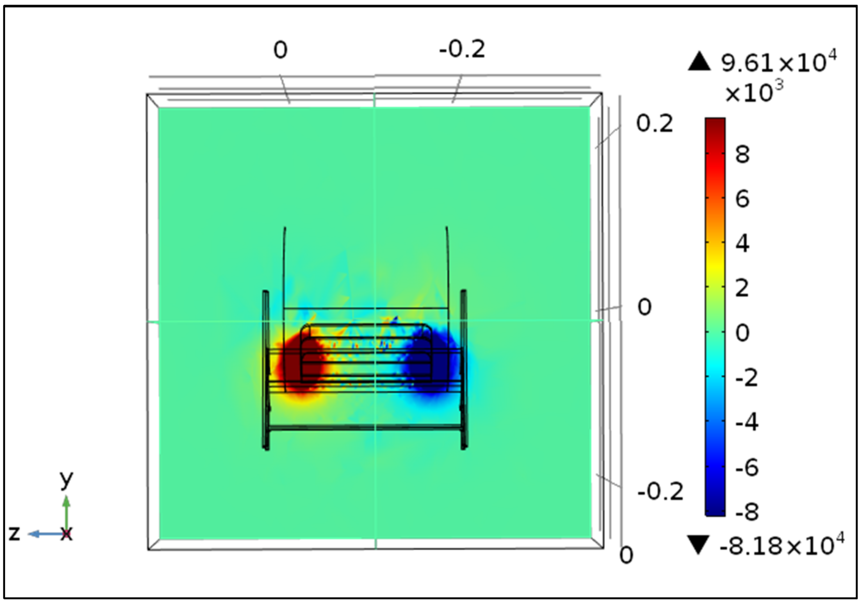

Figure 9. Changes in the magnetic field intensity value in the z-direction (Hz) in the y-z plane in wet LIMS.

4.3. Validation of simulation results of magnetic field

In order to validate the simulation results of the magnetic field, the size of the magnetic field (in Gauss) was measured at 94 points around the magnetic sector using a gauss-meter. Of these, we selected 49 points in the middle section of the magnets and 45 points in the edges of the magnets in 6 directions with different angles and different distances from the magnets (Figure 10). The quantitative comparison of the measured and simulated magnetic field intensity at different points (six different directions at different intervals from the surface of the cylinder shell) is shown in Figure 11 (6 directions and the middle section of the magnet) and Figure 12 (6 directions and edges of the magnets).

As it can be seen in Figure 11, the value for the magnetic field intensity was reduced by an increase in the distance from the cylinder surface, a trend observable in both the laboratory measurement and the results of the simulation. On the other hand, the results of the magnetic field simulation were in agreement with those of laboratory measurement. The results of laboratory measurement and simulation were further compared on the edge of the magnets (Figure 12). In general, the evaluation of Figures11 and 12 showed that the quantitative results of the magnetic field simulation were consistent with the laboratory measurements.

In order to investigate the quantitative adaptability of laboratory measurements and simulation results of magnetic field magnitude, the R squared values of the experimental and simulation curves were separately measured in 6 directions at different distances from the drum surface, and were further added to Figures11 and 12, where the minimum values of R squared for experimental and simulation curves were 0.97 and 0.96, respectively, indicating the high compliance of the laboratory and simulation values.

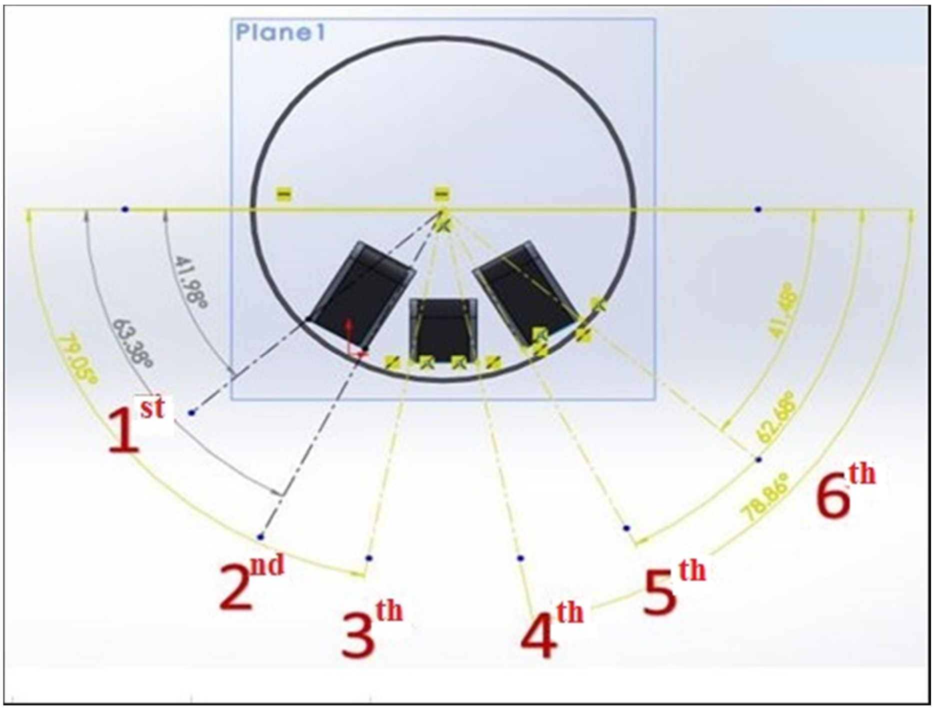

Figure 10. Schematic view of the middle section and the edge of magnets along with directions and selected angles to measure the magnetic field magnitude.

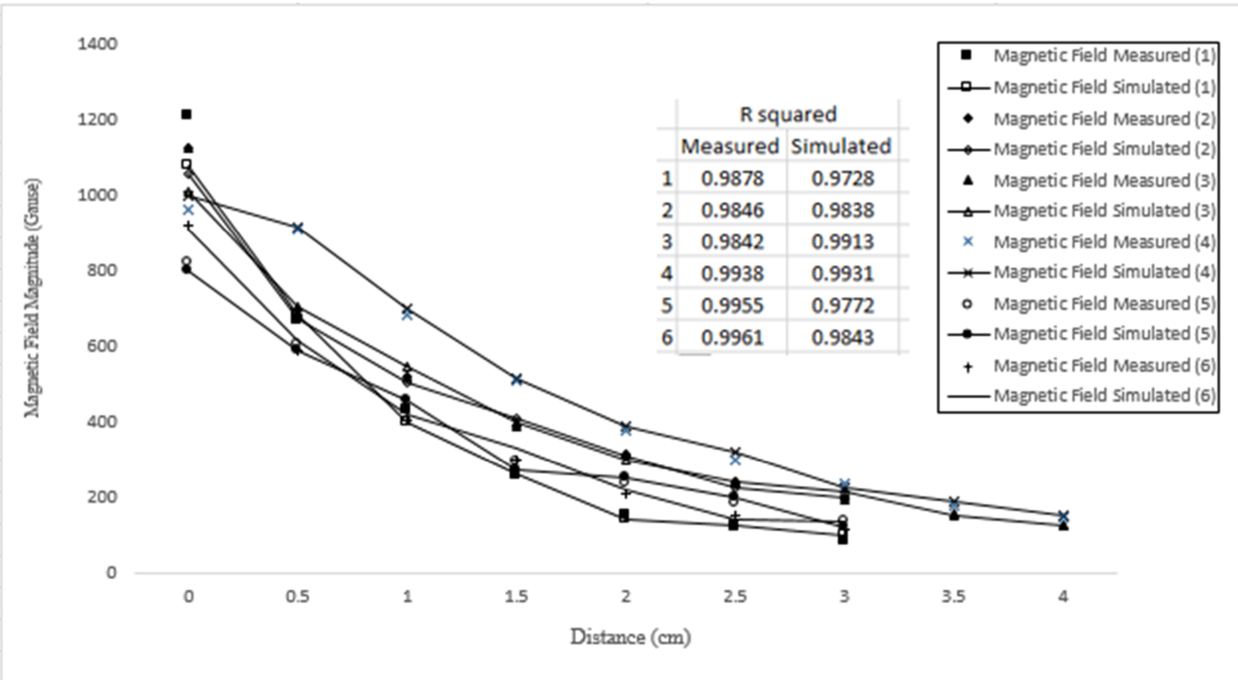

Figure 11. Measured and simulated values of magnetic field magnitude (gauss) in 6 directions and different distances from the surface of the drum in the middle section of the magnets.

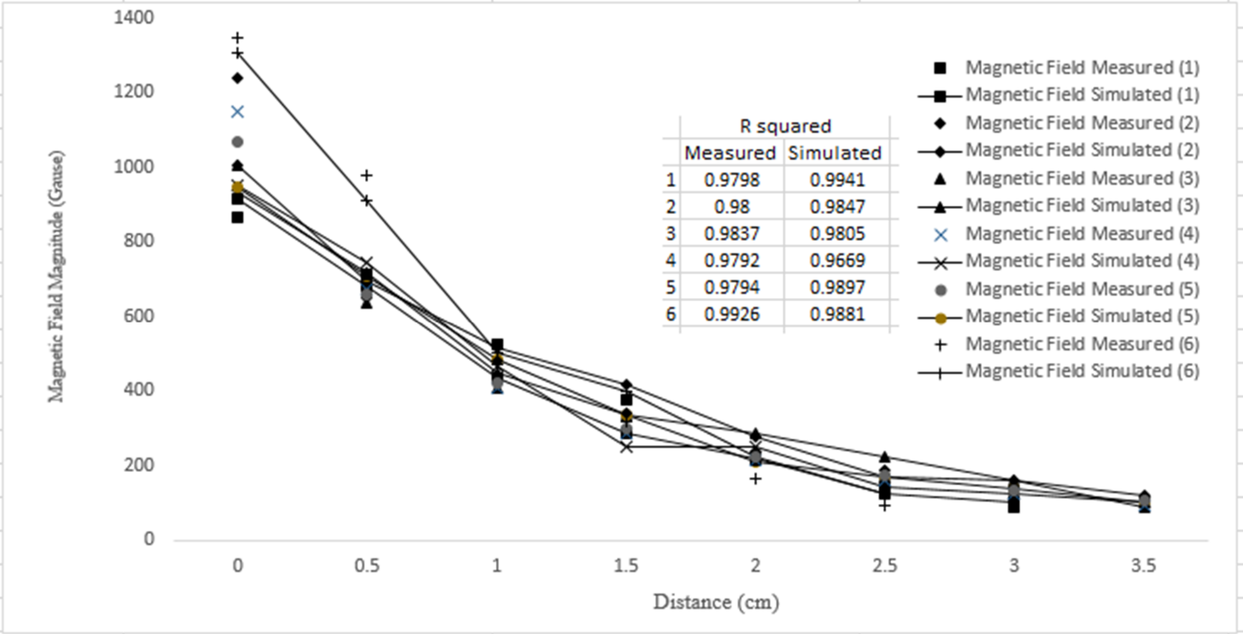

Figure 12. Measured and simulated values of magnetic field magnitude (gauss) in 6 directions and different distances from the surface of the drum at the edge of the magnets.

It is to be noted that the effective magnetic field in the surface of the drum shell and in the middle section of the magnets was about 1,000 gauss (based on the simulation and measurement results, Figure 11), which was slightly higher at the edge of the magnets, about 1100 gauss (Figure 12). This helps increasing the weight recovery of magnetic materials and reduce the waste of magnetic materials in the tailings. Although in the normal mode, the arrangement of the magnets is symmetrically placed inside the cylinder, in certain magnetic separation devices, it is possible to move the magnetic field toward the feed inlet or the outlet of the concentrate. Given the magnitude of the magnetic field, it is clear that if the magnets move towards the feed inlet, the magnitude of the magnetic force applied to the particles increases as a result of an increase in the effective magnetic field intensity, thereby increasing the weight recovery of the product concentrate. Moreover, if the angle of the magnets moves towards the concentrate output, the amount of magnetic force applied to the particles decreases as a result of the effective reduction in the effective magnetic field, hence an increase in the grade of the product of the concentrate.

5. Conclusions

In the present research work, the magnetic variables of the magnetic flux density, intensity of magnetic field, and gradient of the magnetic field intensity were simulated in a drum wet low-intensity magnetic separator using the finite element method (FEM) and employing a COMSOL Multiphysics simulator. Since the magnetic field of the LIMS device is produced with permanent magnets placed inside the drum as an angle form, the AC/DC module and the Magnetic Fields, No Current modeling option in COMSOL Multiphysics were used to simulate the magnetic variables including the magnetic flux density, magnetic field intensity, and gradient of magnetic field intensity. The preliminary simulation results showed that the value of the magnetic flux density on the magnet ranged from 900 to 1000 gauss, and the value of the magnetic field intensity was reduced by an increase in the distance from the cylinder surface. This decreasing trend was obvious in both the laboratory measurement and the results of the simulation. In order to quantitatively validate the simulation results of the magnetic field, the size of the magnetic field was measured at 94 points around the magnetic sector in the middle and at the edge of the magnets. The comparison of the simulation and laboratory measurements showed that the mean value for the simulation error was equal to 9.6%. Moreover, the minimum values of R squared for the experimental and simulation curves were 0.97 and 0.96, respectively, indicating the high compliance of the laboratory and simulations values. Therefore, the performed simulation can be the first step in designing and constructing more developed magnetic separators with higher efficiencies.

Acknowledgments
We are grateful to the Iranian Mines & Mining Industries Development & Renovation (IMIDRO), Iran Mineral Processing Research Center (IMPRC), Gol-Gohar Mining and Industrial Company (GEG), and Golgohar Iron ore and Steel Research Institute (GISRI) for their support, and scientific, technical assistance, and contributions to the work.

References

[1]. Mohanty, S., Das, B. and Mishra, B.K. (2011). A preliminary investigation into magnetic separation process using CFD. Minerals Engineering. 24 (15): 1651-1657.

[2]. Yavuz, C.T., Prakash, A., Mayo, J.T. and Colvin, V.L. (2009). Magnetic separations: from steel plants to biotechnology. Chemical Engineering Science. 64 (10): 2510-2521.

[3]. Das, B., Prakash, S., Bhaumik, S.K., Mohapatra, B.K. and Narasimhan, K.S. (1991). Magnetic separation of iron ore slimes by wet high intensity magnetic separator. Transactions of the Indian Institute of Metals (India). 44 (5): 355-357.

[4]. Song, S., Lu, S. and Lopez-Valdivieso, A. (2002). Magnetic separation of hematite and limonite fines as hydrophobic flocs from iron ores. Minerals engineering. 15 (6): 415-422.

[5]. Arol, A.I. and Aydogan, A. (2004). Recovery enhancement of magnetite fines in magnetic separation. Colloids and Surfaces A: Physicochemical and Engineering Aspects. 232 (2-3): 151-154.

[6]. Chen, L., Xiong, D. and Huang, H. (2009). Pulsating high-gradient magnetic separation of fine hematite from tailings. Mining, Metallurgy & Exploration. 26 (3): 163-168.

[7]. Tripathy, S.K., Banerjee, P.K. and Suresh, N. (2014). Separation analysis of dry high intensity induced roll magnetic separator for concentration of hematite fines. Powder Technology. 264: 527-535.

[8]. Bertrand, C., Bazin, C. and Nadeau, P. (2018). Simulation of a Dry Magnetic Separation Plant. Advances in Metallurgical and Material Engineering. 1 (1): 15-28.

[9]. Svoboda, J. (2004). Magnetic techniques for the treatment of materials. Springer Science & Business Media.

[10]. Iranmanesh, M. and Hulliger, J. (2017). Magnetic separation: its application in mining, waste purification, medicine, biochemistry and chemistry. Chemical Society Reviews. 46 (19): 5925-5934.

[11]. Norrgran, D. (2010). Wet Drum Magnetic Separators for Heavy Media Application, Operation, and Performance. In XVI International Coal Preparation Congress, Lexington: Society for Mining, Metallurgy, and Exploration. pp. 313-319.

[12]. Chen, L., Liao, G., Qian, Z. and Chen, J. (2012). Vibrating high gradient magnetic separation for purification of iron impurities under dry condition. International Journal of Mineral Processing. 102: 136-140.

[13]. Jordens, A., Sheridan, R.S., Rowson, N.A. and Waters, K.E. (2014). Processing a rare earth mineral deposit using gravity and magnetic separation. Minerals Engineering. 62: 9-18.

[14]. Zhang, W., Rezaee, M., Bhagavatula, A., Li, Y., Groppo, J. and Honaker, R. (2015). A review of the occurrence and promising recovery methods of rare earth elements from coal and coal by-products. International Journal of Coal Preparation and Utilization. 35 (6): 295-330.

[15]. Augusto, P.A., Castelo-Grande, T. and Augusto, P. (2005). Magnetic classification in health sciences and in chemical engineering. Chemical Engineering Journal. 111 (2-3): 85-90.

[16]. Alexiou, C., Arnold, W., Klein, R.J., Parak, F.G., Hulin, P., Bergemann, C. and Luebbe, A.S. (2000). Locoregional cancer treatment with magnetic drug targeting. Cancer research. 60 (23): 6641-6648.

[17]. Svoboda, J. and Fujita, T. (2003). Recent developments in magnetic methods of material separation. Minerals Engineering. 16 (9): 785-792.

[18]. Dobbins, M., Dunn, P. and Sherrell, I. (2009, September). Recent advances in magnetic separator designs and applications. In The 7th International Heavy Minerals Conference "What next", The Southern African Institute of Mining and Metallurgy. pp. 63-70.

[19]. Stener, J. (2015). Wet Low-Intensity Magnetic Separation: Measurement methods and Modelling (Doctoral dissertation, Luleå tekniska universitet).

[20]. Dworzanowski, M. (2010). Optimizing the performance of wet drum magnetic separators. Journal of the Southern African Institute of Mining and Metallurgy. 110 (11): 643-653.

[21]. Sido, N.M., Mailfert, A., Gillet, G. and Colteu, A. (2003). Study of high intensity magnetic separation process in grooved plate matrix. The European Physical Journal-Applied Physics. 24 (3): 201-207.

[22]. Okada, H., Mitsuhashi, K., Ohara, T., Whitby, E.R. and Wada, H. (2005). Computational fluid dynamics simulation of high gradient magnetic separation. Separation science and technology. 40 (7): 1567-1584.

[23]. Hayashi, S., Mishima, F., Akiyama, Y. and Nishijima, S. (2010). Development of high gradient

magnetic separation system for removing the metallic wear debris to be present in highly viscous fluid. Physica C: Superconductivity and its applications. 470 (20): 1822-1826.

[24]. Lindner, J., Menzel, K. and Nirschl, H. (2013). Simulation of magnetic suspensions for HGMS using CFD, FEM and DEM modeling. Computers & chemical engineering. 54: 111-121.

[25]. Shaikh, Y.S., Seibert, C. and Kampeis, P. (2016). Study on Optimizing High-Gradient Magnetic Separation—Part 1: Improvement of Magnetic Particle Retention Based on CFD Simulations. World Journal of Condensed Matter Physics. 6 (2): 123.

[26]. Yuan, M., Mo, D., Peng, H. and Wu, D. (2017, October). Magnetic Field Analysis On A Cylindrical Matrix Of HGMS Through Conform Mapping. In 2017 2nd Joint International Information Technology, Mechanical and Electronic Engineering Conference (JIMEC 2017). Atlantis Press.

[27]. Rasool, R. and Lieberwirth, H. (2018). A continuum based numerical modelling approach for the simulation of WHIMS. Minerals Engineering. 118: 97-105.

[28]. Murariu, V. (2013). Simulating a low intensity magnetic separator model (LIMS) using DEM, CFD and FEM magnetic design software. In The 4th International Computational Modelling Symposium, Cornwall: Minerals Engineering International. pp. 301-314.

[29]. Zhe, J.I.N., Xin, T.A.N.G. and Wang, W.M. (2006). A Method for Shimming a Permanent Magnet with FEA. Journal of Iron and Steel Research, International. 13: 423-426.

[30]. LIU, J.F., Choi, H. and Walmer, M. (2006). Design of permanent magnet systems using finite element analysis. Journal of Iron and Steel Research, International. 13: 383-387.

[31]. Lozin, A.A., Nitiagovsky, V.V. and Hud, V.N. (2006). Magnetic System with “Antiradial” Magnetization. Journal of Iron and Steel Research, International. 13: 471-473.

[32]. Wimmer, G., Clemens, M. and Lang, J. (2008). Calculation of magnetic fields with finite elements. In From Nano to Space, Springer, Berlin, Heidelberg. pp. 111-124.

[33]. Manz, B., Benecke, M. and Volke, F. (2008). A simple, small and low cost permanent magnet design to produce homogeneous magnetic fields. Journal of magnetic resonance. 192 (1): 131-138.

[34]. Smolkin, M.R. and Smolkin, R.D. (2006). Calculation and analysis of the magnetic force acting on a particle in the magnetic field of separator. Analysis of the equations used in the magnetic methods of separation. IEEE Transactions on Magnetics. 42 (11): 3682-3693.

[35]. Knoll, J. and Nirschl, H. (2014). Influence of the magnetic force on the van der Waals force of super paramagnetic composite particles. Powder Technology. 259: 30-36.

[36]. Luo, L. and Nguyen, A.V. (2017). A review of principles and applications of magnetic flocculation to separate ultrafine magnetic particles. Separation and Purification Technology. 172: 85-99.

[37]. U.S. Patents, (2013). “Multiphysics Modeling using COMSOL”, Available at www.comsol.com/product-download.

شبیه‌سازی توزیع میدان مغناطیسی با استفاده از روش مدل‌سازی المان محدود و مطالعات آزمایشگاهی در جداکننده مغناطیسی شدت پایین تر

پویا کریمی[۱]، احمد خدادادی دربان[۱*] و زهرا منصورپور[۲]

۱- بخش مهندسی معدن، دانشگاه تربیت مدرس، ایران
۲- بخش مهندسی شیمی، دانشکده فنی و مهندسی، دانشگاه تهران، ایران

ارسال ۲۰۱۹/۲/۲۳، پذیرش ۲۰۱۹/۶/۲۵

* نویسنده مسئول مکاتبات: akdarban@modares.ac.ir

چکیده:

جداکننده‌های مغناطیسی شدت پایین به طور گسترده‌ای در تحقیقات و صنعت استفاده می‌شوند. پیشرفت در تکنیک‌های جداسازی مغناطیسی منجر به گسترش استفاده از این روش در زمینه‌های مختلف مانند فرآوری مواد معدنی مغناطیسی، تصفیه فاضلاب و انتقال دارو در بدن انسان شده است. در صنعت فرآوری مواد معدنی، کاربرد اصلی جدایش مغناطیسی تر از طریق استفاده از جداکننده‌های مغناطیسی استوانه‌ای امکان‌پذیر می‌باشد. طراحی این جداکننده بر اساس چرخش استوانه در داخل یک مخزن می‌باشد، به‌گونه‌ای که مجموعه‌ای از آهنرباهای دائمی به شکل زاویه‌ای درون استوانه قرار گرفته (قطاع مغناطیسی) و یک میدان مغناطیسی تولید می‌کنند. در این پژوهش، متغیرهای مغناطیسی شامل (چگالی شار مغناطیسی، شدت میدان مغناطیسی و گرادیان شدت میدان مغناطیسی) در جداکننده مغناطیسی شدت پایین تر آزمایشگاهی با استفاده از روش عددی المان محدود و شبیه‌ساز COMSOL Multiphysics شبیه‌سازی شده است؛ در ادامه متغیرهای شبیه‌سازی‌شده از طریق اندازه‌گیری‌های آزمایشگاهی اعتبارسنجی شده است. مقایسه بین نتایج شبیه‌سازی و اندازه‌گیری‌های آزمایشگاهی (میدان مغناطیسی) نشان داد که میانگین مقدار خطای شبیه‌سازی در ۹۴ نقطه در ۲ مقطع اندازه‌گیری برابر با ۹/۶٪ بوده است. علاوه بر این، حداکثر خطای شبیه‌سازی در مقطع وسطی آهنرباهای دائمی موجود در استوانه دستگاه جداکننده، به عنوان مهم‌ترین بخش تولید میدان مغناطیسی در فرآیند جداسازی مغناطیسی، در راستای ششم اندازه‌گیری‌ها و برابر ۷/۸٪ بوده است؛ بنابراین، شبیه‌سازی انجام شده می‌تواند به عنوان نخستین گام برای طراحی و ساخت جداکننده‌های مغناطیسی پیشرفته‌تر استفاده شود.

کلمات کلیدی: جدایش مغناطیسی، جداکننده مغناطیسی استوانه‌ای تر، شبیه‌سازی میدان مغناطیسی، روش المان محدود.